Three-dimensional simulations of the complex dielectric properties of random composites by finite element method

Xuanhe Zhao, Yugong Wu,[a] Zhigang Fan, and Fei Li
School of Electronic and Information Engineering, Tianjin University, Tianjin 300072, People's Republic of China

(Received 5 May 2003; accepted 29 February 2004)

Complex dielectric constants of binary-phase random composites are simulated for a three-dimensional structure consisting of cubic grains using the Monte Carlo-finite element method. Numerical results are fitted using Maxwell–Garnett, Bruggeman symmetrical, and general effective media formulas, and the fitting efficiencies of the formulas are quantitatively evaluated. The general effective media formula gives the best fitting to our simulation results and its accuracy is better than 3.7%. The effects of frequencies on the spatial distribution of electrostatic potentials in dielectric composites are discussed. The distribution of potential contours drawn in the low-frequency region and the high-frequency region show great variation, because of different lengths of time for charge to accumulate near the interphase boundaries. Dielectric spectra are drawn by varying volume fraction and lossy property of one phase in binary-phase composites. General properties of the dielectric spectra are discussed and the characteristics of the dielectric spectra caused by the differences in the lossy properties of the two phases at certain volume fractions are analyzed. [DOI: 10.1063/1.1712017]

I. INTRODUCTION

Composite materials have been extensively used in electrical applications. The fact that they are often made up of at least two constituents or phases enables us to tailor materials for special purposes. The electrical properties of a composite system are determined by the properties of the constituents, interaction between them, and geometrical configuration. In designing composite materials with specified properties for electrical applications, one should take these parameters into consideration. Typical experimental design methods are characterized by a classical ''trial and error'' approach.[1] The modeling and simulations of desired properties of composite systems can offer quick predictions and provide valuable advice for material designers, especially when high performance computers have become accessible.

The modeling of dielectric properties of insulation systems has received considerable fundamental attention in recent years. For example, Sereni *et al.*[2] have published a series of articles on the modeling of complex effective permittivity by finite element method (FEM) and boundary integral equation method, simulating both dielectric constants and losses for a periodic binary-phase composite material.[2] However, for composites with a random structure, they only calculated the dielectric constants without losses.[2] Krakovaky and Myroshnychenko[3] and Tuncer[4] simulated both dielectric constants and losses of random binary-phase composite materials using two-dimensional (2D) models. Ang *et al.* calculated the dielectric constants and losses of binary-phase composites that consisted of phase *a* with different shapes (circles and triangles) distributed in a matrix phase *b*.[5] Their models were also two-dimensional.[5] Tuncer *et al.*[1] gave an excellent review of the property and modeling of dielectric mixtures, finding that three-dimensional (3D) structural simulations still need development. In this article, we simulate the complex dielectric properties of lossy composites with a 3D structure using a Monto Carlo-finite element method (MC-FEM).

This article is organized as follows. In Sec. II, we propose our numerical model and the basic theories underlying it. In Sec. III, a brief summary of the dielectric mixture formulas used for the comparison with the numerical results follows. In Sec. IV, the MC-FEM results are compared with the predictions of mixture formulas, and also analyzed in other approaches. Section V contains concluding remarks of this work.

II. MODELING

A. Basic theory

In dielectric matter, the relation between dielectric displacement $\bar{D}$ and applied electric field $\bar{E}$ is often linear and can be expressed as the following equation:

$$\bar{D}=\epsilon_0\epsilon\bar{E}, \tag{1}$$

where the relative permittivity ϵ describes the dielectric properties of the matter and constant $\epsilon_0=1/36\pi(nF/m)$ is the permittivity of free space.

According to Maxwell equations, $\bar{D}$ obeys

$$\nabla\times\bar{D}=\rho, \tag{2}$$

where ρ is the volumetric charge density.

The continuity equation is

$$\nabla\times\bar{J}=-\partial\rho/\partial t, \tag{3}$$

[a]Electronic mail: wuyugong@yahoo.com.cn

where $\bar{J}$ is current density.

Substituting Eq. (2) into Eq. (3) gives

$$\nabla\left(\bar{J}+\frac{\partial\bar{D}}{\partial t}\right)=0. \tag{4}$$

Using Eqs. (1) and (4), and Ohm's Law

$$\bar{J}=\sigma\bar{E} \tag{5}$$

we have

$$\nabla\left(\sigma\bar{E}+\frac{\partial}{\partial t}\epsilon_0\epsilon\bar{E}\right)=0, \tag{6}$$

where σ is conductivity of the material.

In the case of sinusoidal $\bar{E}$ of angular frequency ω, Eq. (6) becomes

$$\nabla(\sigma+i\omega\epsilon_0\epsilon)\bar{E}=0. \tag{7}$$

When the dielectric losses are assumed to be purely ohmic, i.e.,

$$\epsilon''=\frac{\sigma}{\epsilon_0\omega} \tag{8}$$

and ϵ in Eq. (7) is written into the form of ϵ', Eq. (7) becomes

$$\nabla(\epsilon'-i\epsilon'')\omega\bar{E}=0. \tag{9}$$

When ϵ' and σ are assumed to be frequency independent, Eq. (9) becomes

$$\nabla\times\epsilon\bar{E}=0, \tag{10}$$

where $\epsilon=\epsilon'-\epsilon''i$ is called complex relative dielectric constants of that medium.

When the dielectric material is nonmagnetic (magnetic permeability $\mu=1$) and ω is low enough to neglect the interaction between the magnetic and electric fields, the gradient of electric scalar potential is

$$\nabla\Phi=-\bar{E}. \tag{11}$$

Substituting Eq. (11) into Eq. (10) gives

$$\nabla\times\epsilon\nabla\Phi=0 \tag{12}$$

the resolution of which under specific boundary conditions forms the basis of our numerical model.

B. Numerical model

Our simulation of the effective complex dielectric constants of binary-phase composites is performed on the model as shown in Fig. 1. A parallel plate capacitor, with conducting planes of areas S and separation h is filled with a statistically isotropic composite dielectric, consisting of two isotropic lossy materials with complex dielectric constants ϵ_a and ϵ_b (or with real dielectric constants ϵ_a' and ϵ_b', and conductivity σ_a and σ_b). A harmonically oscillating potential difference $U=U_0\exp(i\omega t)$ is applied on this capacitor with an angular frequency ω. The two phases in this composite are composed of cubic grains, designated as phase *a* or phase *b* by standard Monte Carlo method using random number generator, bounded by the volume fraction of each phase.

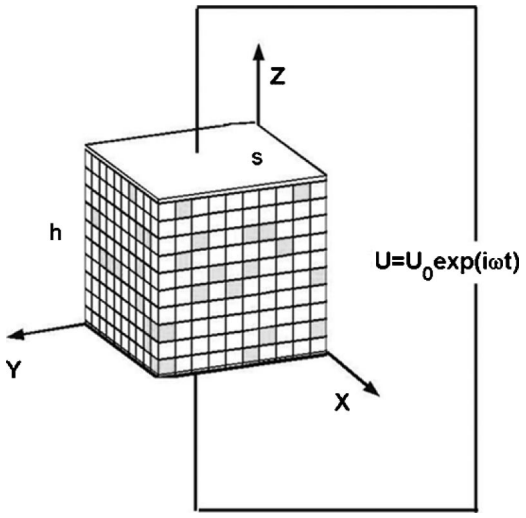

FIG. 1. A parallel plate capacitor filled with a dielectric composite consisting of two phases: *a* (gray cubic grain) and *b* (white cubic grain). The finite element lattice in this illustration is 10×10×10.

Therefore, the two phases in this composite have similar morphologies and are distributed randomly through the whole system.

The problem we face is to solve Eq. (12) in conjunction with boundary conditions

$$\Phi=U_0\exp(i\omega t) \quad \text{on the top plane,} \tag{13}$$

$$\Phi=0 \quad \text{on the bottom plane,} \tag{14}$$

and continuity conditions on the interface boundaries of the two phases

$$\Phi_a=\Phi_b, \tag{15}$$

$$\epsilon_a\bar{n}\times\nabla\Phi_a=\epsilon_b\bar{n}\times\nabla\Phi_b, \tag{16}$$

where $\bar{n}$ is the unit vector normal to the interface.

The elimination of fringing effects

$$\bar{n}\times\nabla\Phi=0 \quad \text{on the side planes} \tag{17}$$

also has to be satisfied. Here $\bar{n}$ is normal to the side surface considered.

Using FEM, we split the composite model shown in Fig. 1 into N_e finite elements by means of N nodes. The largest node number in this paper is about 360 000. The potential distribution in this space can be approximated inside each element using interpolation functions.[6] By solving the matrix equations resulting from this discretization procedure, we obtain the potential and its normal derivation on each node of the mesh.

Based on this potential distribution, we compute both the electrostatic stored energy and dielectric loss on each element of the mesh. The energy stored in the capacitor as shown in Fig. 1 can be evaluated as[2]

$$W_e=\frac{1}{2}\epsilon_0\epsilon'\frac{S}{h}U_0^2, \tag{18}$$

and energy loss as[2]

$$\rho = \frac{1}{2}\epsilon_0 \epsilon'' \frac{S}{h}\omega U_0^2. \tag{19}$$

Thus, the real and imaginary parts of the effective complex dielectric constants of this system can be obtained.

More details of FEM applications to electrical composite systems can be found in Refs. 1–6.

III. DIELECTRIC MIXING RULES

For composite materials, one of the challenging problems of both theoretical and practical importance has been the prediction and computation of the effective electrical properties. A variety of mixture formulas have been proposed based on different theories.[7–14] Bergman and Stroud gave an excellent review of the physical properties of composite media for this problem.[15]

Effective medium theory considers the dielectric or electric response of a heterogeneous system by assuming that each particle or unit is, on average, surrounded by a mixture, which has the assumed homogenous media.[7]

Maxwell–Garnett formula can be expressed by[8]

$$\epsilon_m = \epsilon_b \frac{\epsilon_b V_b(1-K) + \epsilon_a(V_a + KV_b)}{\epsilon_b + KV_b(\epsilon_a - \epsilon_b)}. \tag{20}$$

Here $\epsilon_a = \epsilon_a' - \epsilon_a'' i$ and $\epsilon_b = \epsilon_b' - \epsilon_b'' i$ are the complex dielectric constants of phase a and phase b, V_a, and V_b are the volume fractions ($V_a + V_b = 1$), and $\epsilon_m = \epsilon_m' - \epsilon_m'' i$ is the effective complex dielectric constant of the composite. The depolarization factor of the particles of phase a in the direction perpendicular to the capacitor plates is K. Maxwell–Garnett formula is generally valid for composites composed of a small volume fraction of particles (phase a) randomly dispersed into a host matrix (phase b). Bruggeman symmetrical formula for the dielectric constants of binary-phase composite materials can be written as[9,10]

$$\frac{V_a(\epsilon_a - \epsilon_m)}{\epsilon_a + A\epsilon_m} + \frac{V_b(\epsilon_b - \epsilon_m)}{\epsilon_b + A\epsilon_m} = 0. \tag{21}$$

The nonfixed parameter A can be expressed as

$$A = \frac{1-\phi_c}{\phi_c}. \tag{22}$$

Here ϕ_c is the critical volume fraction of phase a. Because the Bruggeman symmetrical formula treats both phases on a completely symmetrical basis, it is expected to be more applicable to the media where both phases have similar morphologies and are randomly distributed through the whole system.

Both the Maxwell–Garnett and Bruggeman symmetrical formulas are based on effective media theory. It is worth noting that effective media theory is insensitive to the detailed structures of composite materials, for example, the connectedness and clustering of one phase in a binary-phase random composite.[11]

Percolation theory describes a phenomenological power-law dependence for the conductivity of a mixture near the conductor-insulator transition.[12,13] Strictly speaking, percolation theory is valid only when the ratio of the conductivity or resistivity of the two phases in a binary-phase composite approaches infinity. This limits the application of percolation theory to many real heterogeneous systems, particularly dielectric systems.

Combining percolation considerations into effective medium theory, McLachlan proposed a general effective medium (GEM) formula[14]

$$\frac{V_a(\epsilon_a^{1/t} - \epsilon_m^{1/t})}{\epsilon_a^{1/t} + A\epsilon_m^{1/t}} + \frac{V_b(\epsilon_b^{1/t} - \epsilon_m^{1/t})}{\epsilon_b^{1/t} + A\epsilon_m^{1/t}} = 0. \tag{23}$$

The GEM formula has two nonfixed parameters A and t to characterize the microstructure or distribution and interconnectivity of the components in composite materials. Here A is also related to ϕ_c by Eq. (22). The GEM formula reduces to the Bruggeman symmetrical formula when $t=1$ and has the mathematical form of the percolation model in certain limits.

IV. RESULTS AND DISCUSSION

A. Accuracy of the algorithm

The effective complex dielectric constants of a serial mixing system can be calculated precisely by Lichtenecker's serial mixing rule[16]

$$\frac{1}{\epsilon_m} = \frac{V_a}{\epsilon_a} + \frac{V_b}{\epsilon_b}. \tag{24}$$

We have performed FEM calculations on serial mixing system with $\epsilon_a = 6-5i$ and $\epsilon_b = 4-3i$, using the algorithm described in Sec. II without Monte Carlo method. Through comparison, we find that the deviations of both real and imaginary parts of the effective complex dielectric constants simulated by FEM from the theoretical ones are less than 1×10^{-12}. This demonstrates the accuracy of our algorithm for computing the complex dielectric constants of three-dimensional lossy composites.

B. Numerical results fitted by the formulas

Using the model described in Sec. II, we simulated the effective complex dielectric constants of four binary-phase

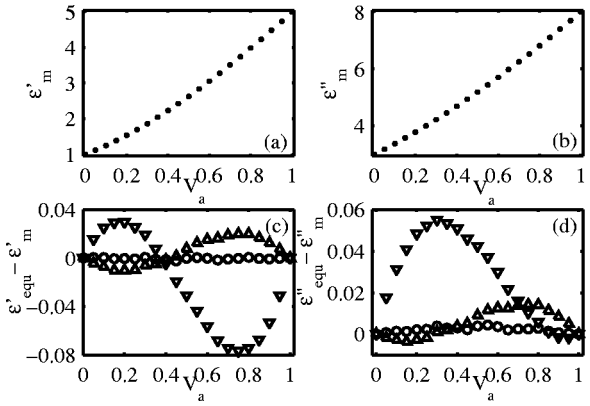

FIG. 2. The effective complex dielectric constants simulated by MC-FEM (●) and the deviations of the predictions of Maxwell–Garnett (▽), Bruggeman symmetrical (△), and GEM (○) formulas from MC-FEM values for $\epsilon_a = 5-8i$ and $\epsilon_b = 1-3i$.

composite systems: $\epsilon_a=5-8i\ \epsilon_b=1-3i$, $\epsilon_a=8-3i\ \epsilon_b=3-1i$, $\epsilon_a=3-0.03i\ \epsilon_b=1-0.00i$, and $\epsilon_a=500\ \epsilon_b=1$. In each system, V_a ranges from 0.05 to 0.95 at equal intervals of 0.05. For each V_a, we take the average of 200 MC-FEM calculations as the effective dielectric constant ϵ_m. This provides values of the effective permitivities and dielectric losses, with a coefficient of variation (e.g. standard deviation divided by average) less than 4%.

The dielectric mixture formulas discussed in Sec. III are fitted to ϵ_m's of each composite system. The quantity

$$\delta=\sqrt{\frac{\Sigma_n\{C'[(\epsilon'_m-\epsilon'_{\mathrm{equ}})/0.01\epsilon'_m]^2+C''[(\epsilon''_m-\epsilon''_{\mathrm{equ}})/0.01\epsilon''_m]^2\}}{n-p}} \tag{25}$$

is minimized by varying the nonfixed parameters in dielectric mixture formulas,[14,17] where $\epsilon'_m-\epsilon''_m i=\epsilon_m$ is the effective complex dielectric constant simulated by MC-FEM, and $\epsilon'_{\mathrm{equ}}-\epsilon''_{\mathrm{equ}}i=\epsilon_{\mathrm{equ}}$ the effective complex dielectric constant calculated by dielectric mixture formulas, n the number of data points (here $n=19$), p the number of variable parameters in dielectric mixture formulas, and C' C'' are weighting factors. If $\delta=1$, the data of this system could be fitted to an accuracy of 1%. The algorithm for minimizing δ is based on the solution of corresponding Kuhn–Tucker equation through sequential quadratic method.[18] This fitting technique has been widely used for fitting the predictive formulas to experimental results of both conductivity[14] and dielectric constants.[17]

For systems of $\epsilon_a=5-8i\ \epsilon_b=1-3i$, $\epsilon_a=8-3i\ \epsilon_b=3-1i$, and $\epsilon_a=3-0.03i\ \epsilon_b=1-0.00i$, C' and C'' are chosen to be 0.5 equally. For system of $\epsilon_a=500\ \epsilon_b=1$, C' is set equal to 1 with C'' equal to 0, as ϵ''_m has a value of zero. In Figs. 2–5, we show the effective complex dielectric constants simulated by MC-FEM for the four systems. For comparison, the deviations of the predictions of Maxwell–Garnett, Bruggeman symmetrical, and GEM formulas from MC-FEM values are also plotted in Figs. 2–5. It can be observed that the deviations of GEM formula's predictions from MC-FEM values are very slight. On the other hand, Maxwell–Garnett and Bruggeman symmetrical formulas have much greater deviations from MC-FEM values, with the deviations from Maxwell–Garnett formalism being the greatest. The origin is due to (1) in each of the four composite systems, the volume fractions of both phase *a* and phase *b* are ranging from 0.05 to 0.95, but Maxwell–Garnett formula is valid when there is only a very small volume fraction of one component and (2) neither Maxwell–Garnett formula nor Bruggeman symmetrical formula consider the connectedness or clustering of individual phases in composites.[11] However, the connectivity property can significantly affect the effective permitivities and losses of our MC-FEM model at certain composition range.

To quantitatively check the fitting efficiency of Maxwell–Garnett, Bruggeman symmetrical, and GEM formulas, we show the δ values obtained by fitting them to MC-FEM results, in Table I. It is obvious that the δ values for GEM formula are much smaller than those for Maxwell–Garnett and Bruggeman symmetrical formulas. It can be found that the fitting of the GEM formula to our numerical results has an accuracy better than 3.7%. In fact, the GEM formula can also satisfactorily model the dielectric constants of some composite systems such as PMN-pyrochlore,[17] over its entire composition range. Despite its fitting accuracy, GEM formula needs two nonfixed parameters (i.e., A and t) to characterize the microstructure or distribution and interconnectivity of the components of composites. Therefore, in order to calculate the parameters of GEM formula for a composite system, one needs *a prior* information on that system.

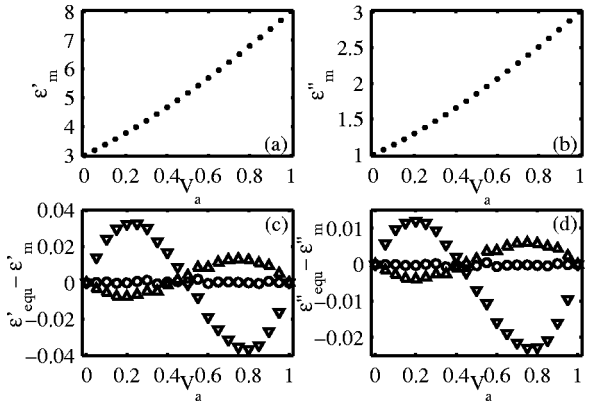

FIG. 3. The effective complex dielectric constants simulated by MC-FEM (●) and the deviations of the predictions of Maxwell–Garnett (▽), Bruggeman symmetrical (△), and GEM (○) formulas from MC-FEM values for $\epsilon_a=8-3i$ and $\epsilon_b=3-i$.

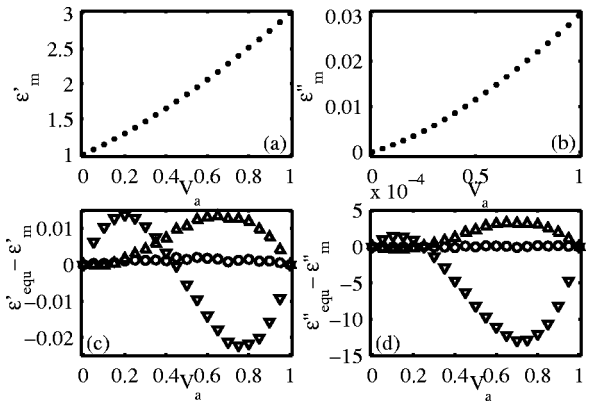

FIG. 4. The effective complex dielectric constants simulated by MC-FEM (●) and the deviations of the predictions of Maxwell–Garnett (▽), Bruggeman symmetrical (△), and GEM (○) formulas from MC-FEM values for $\epsilon_a=3-0.03i$ and $\epsilon_b=1-0.00i$.

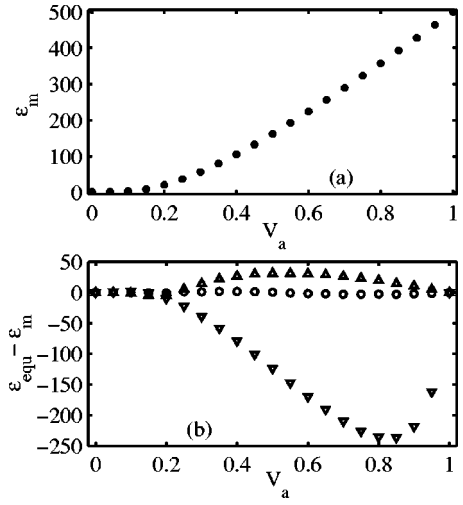

FIG. 5. The effective complex dielectric constants simulated by MC-FEM (●) and the deviations of the predictions of Maxwell–Garnett (▽), Bruggeman symmetrical (△), and GEM (○) formulas from MC-FEM values for $\epsilon_a = 500$ and $\epsilon_b = 1$.

C. Potential distribution

When a harmonically oscillating dielectric field is applied on dielectric composites at low frequencies, one effect often observed as a result of the difference in dielectric properties of the components is the accumulation of the charge carriers near the interphase boundaries. This effect is known as the interfacial or Maxwell–Wagner–Sillars polarization. Interfacial polarization can cause the undulation of spatial distribution of the amplitudes of potentials in composites. Illustrating this point, a dielectric composite system with 0.2 volume fraction of phase *a* is chosen. The dielectric constants and ohmic conductivities of phase *a* and phase *b* are $\epsilon_a' = 5$ $\epsilon_b' = 2$ and $\sigma_a = 3 \times 10^{-6}\ \mathrm{Sm}^{-1}$ $\sigma_b = 5 \times 10^{-10}\ \mathrm{Sm}^{-1}$, respectively. A harmonically oscillating potential difference is applied to this system with an angular frequency $\omega = 10\ \mathrm{rad\,s}^{-1}$, resulting in a distribution of the potential amplitudes in the composite. In Fig. 6, we show the potential contours on the section planes vertical to *X* and *Y* axes. It is evident that potential contours on these sections tends to distribute in such a manner as to avoid passing through phase *a*. The undulation of the distribution of the amplitudes of the potentials is obvious. On the other hand, as the frequency rises to $\omega = 10^8\ \mathrm{rad\,s}^{-1}$, this undulation becomes smooth and slight as shown in Fig. 7. In this case, the period of potential oscillation is not sufficient enough for the charge to accumulate near the inter-phase boundaries.

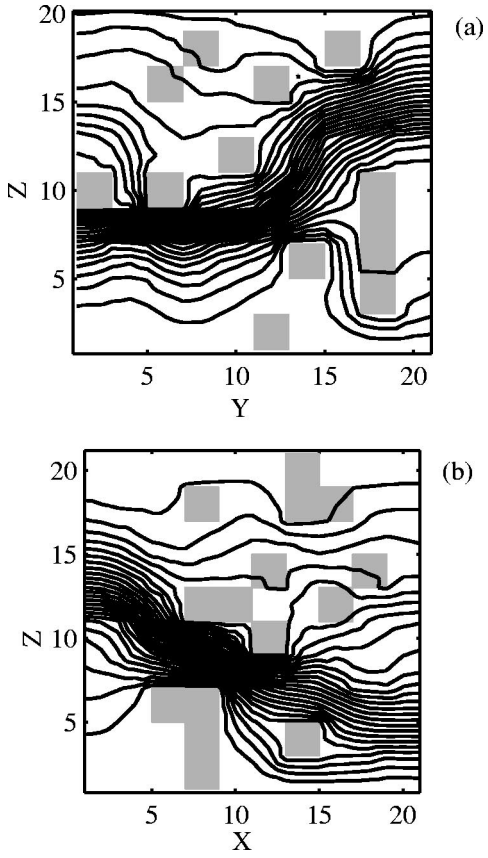

FIG. 6. Potential contours on section planes (a) $X = 9$ and (b) $Y = 9$ at low frequency ($\omega = 10\ \mathrm{rad\,s}^{-1}$). The permittivities and ohmic conductivities of phase *a* (gray cells) and phase *b* are $\epsilon_a' = 5$ $\sigma_a = 10^{-6}\ \mathrm{Sm}^{-1}$ and $\epsilon_b' = 2$ $\sigma_b = 10^{-10}\ \mathrm{Sm}^{-1}$, respectively. The volume fraction of phase *a* is 0.2.

TABLE I. The δ values and parameters of GEM, Bruggeman symmetrical, and Maxwell–Garnett formulas fitted to the MC-FEM results.

Composite	δ			Parameter		
	GEM	Bruggeman symmetrical	Maxwell–Garnett	GEM	Bruggeman symmetrical	Maxwell–Garnett
$\epsilon_a = 5 - 8i$ $\epsilon_b = 1 - 3i$	0.0477	0.3411	1.2797	$t = 1.176$ $A = 3.133$ $(\phi_c = 0.243)$	$A = 2.613$ $(\phi_c = 0.277)$	$K = 0.176$
$\epsilon_a = 8 - 3i$ $\epsilon_b = 3 - 1i$	0.0153	0.1817	0.6403	$t = 1.176$ $A = 3.108$ $(\phi_c = 0.244)$	$A = 2.572$ $(\phi_c = 0.280)$	$K = 0.188$
$\epsilon_a = 3 - 0.03i$ $\epsilon_b = 1 - 0.00i$	0.0970	1.2751	4.6968	$t = 1.176$ $A = 3.133$ $(\phi_c = 0.242)$	$A = 2.805$ $(\phi_c = 0.263)$	$K = 0.183$
$\epsilon_a = 500$ $\epsilon_b = 1$	3.6714	21.1596	71.2710	$t = 1.290$ $A = 5.601$ $(\phi_c = 0.151)$	$A = 4.321$ $(\phi_c = 0.188)$	$K = 0.023$

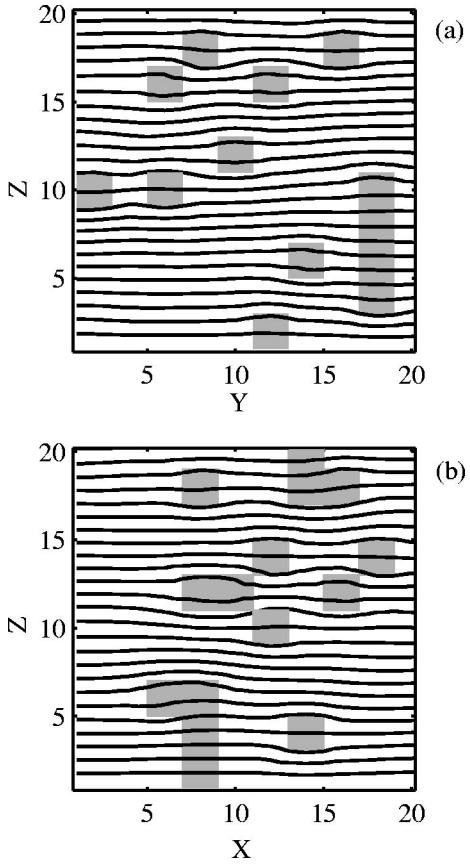

FIG. 7. Potential contours on section planes (a) $X=9$ and (b) $Y=9$ at high frequency ($\omega=10^8$ rad s^{-1}). The permittivities and ohmic conductivities of phase a (gray cells) and phase b are $\epsilon_a'=5$, $\sigma_a=10^{-6}$ Sm^{-1} and $\epsilon_b'=2$, $\sigma_b=10^{-10}$ Sm^{-1}, respectively. The volume fraction of phase a is 0.2.

D. Dielectric spectra

In this section, we analyze the dielectric spectra for a lossy composite system with phase a and phase b, as shown in Fig. 1. The volume fraction of phase a (V_a) is chosen to be 0.05, 0.10, 0.15, 0.20, 0.50, and 0.80, respectively. For each volume fraction, the microstructure of the composite is fixed. The permittivities and ohmic conductivities of phase a and phase b are taken as $\epsilon_a'=5$, $\sigma_a=10^{-6}$ Sm^{-1} and $\epsilon_b'=2$, $\sigma_b=10^{-8}$ Sm^{-1}, 10^{-10} Sm^{-1}, or 10^{-11} Sm^{-1}, respectively. At each V_a, three dielectric spectra are drawn for different σ_b's. These dielectric spectra are shown in Figs. 8–13, respectively.

It can be observed that all the plots of ϵ_m' versus $\log(\omega)$ have a similar shape, characterized by a flat-sharp-flat decrease of ϵ_m' [Figs. 8(a)–13(a)]. In the low-frequency region, lower σ_b results in the greater ϵ_m', at constant V_a. For $V_a=0.15$ [Fig. 10(a)], the difference between ϵ_m' values for $\sigma_b=10^{-8}$ Sm^{-1} and 10^{-11} Sm^{-1} is the greatest. The plots of ϵ_m' versus $\log(\omega)$ show little frequency dependence in the high-frequency region, and ϵ_m''s for different σ_b values nearly have no difference.

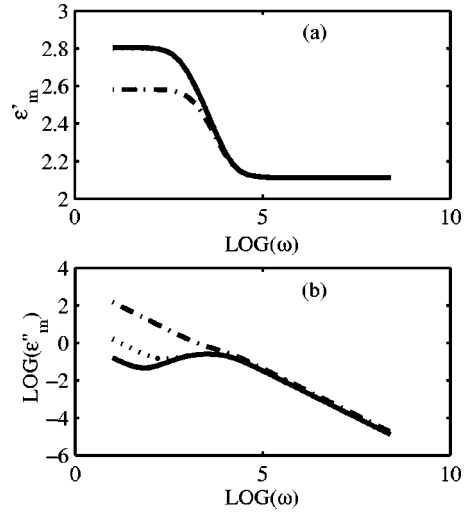

FIG. 8. Dielectric spectra of the composite at $V_a=0.05$ calculated by MC-FEM for $\epsilon_a'=5$, $\sigma_a=10^{-6}$ Sm^{-1} and $\epsilon_b'=2$, $\sigma_b=10^{-8}$ Sm^{-1} (dot-dashed line), 10^{-10} Sm^{-1} (dotted line), or 10^{-11} Sm^{-1} (solid line), respectively.

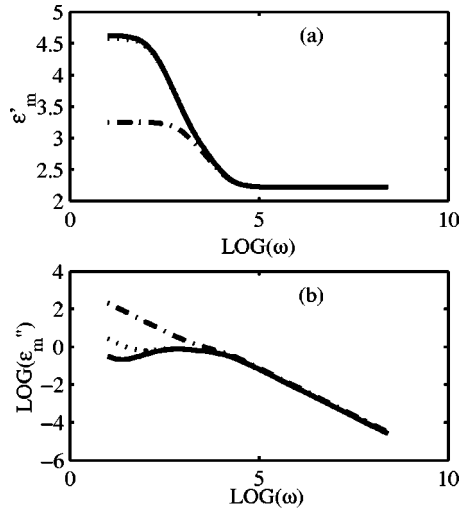

FIG. 9. Dielectric spectra of the composite at $V_a=0.10$ calculated by MC-FEM for $\epsilon_a'=5$, $\sigma_a=10^{-6}$ Sm^{-1} and $\epsilon_b'=2$, $\sigma_b=10^{-8}$ Sm^{-1} (dot-dashed line), 10^{-10} Sm^{-1} (dotted line), or 10^{-11} Sm^{-1} (solid line), respectively.

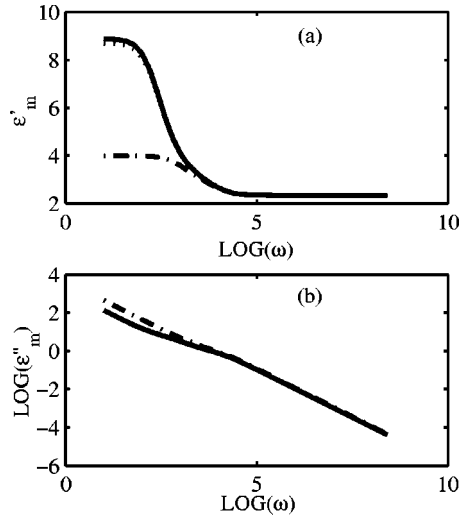

FIG. 10. Dielectric spectra of the composite at $V_a=0.15$ calculated by MC-FEM for $\epsilon_a'=5$, $\sigma_a=10^{-6}$ Sm^{-1} and $\epsilon_b'=2$, $\sigma_b=10^{-8}$ Sm^{-1} (dot-dashed line), 10^{-10} Sm^{-1} (dotted line), or 10^{-11} Sm^{-1} (solid line), respectively.

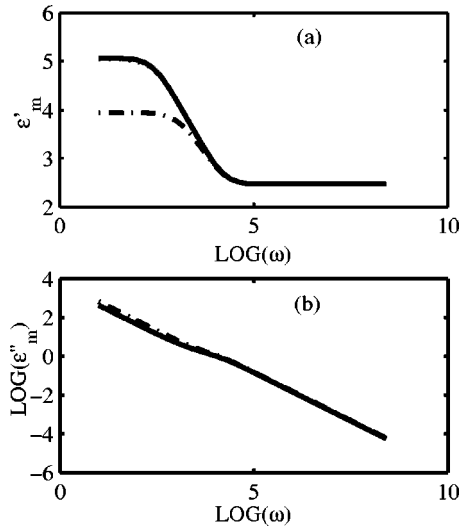

FIG. 11. Dielectric spectra of the composite at $V_a=0.20$ calculated by MC-FEM for $\epsilon_a'=5$, $\sigma_a=10^{-6}\,\mathrm{Sm}^{-1}$ and $\epsilon_b'=2$, $\sigma_b=10^{-8}\,\mathrm{Sm}^{-1}$ (dot-dashed line), $10^{-10}\,\mathrm{Sm}^{-1}$ (dotted line), or $10^{-11}\,\mathrm{Sm}^{-1}$ (solid line), respectively.

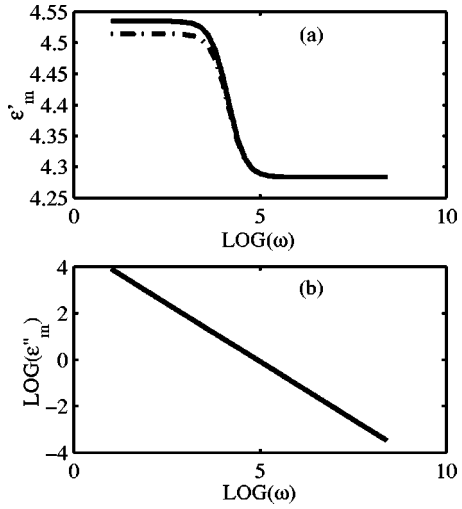

FIG. 13. Dielectric spectra of the composite at $V_a=0.80$ calculated by MC-FEM for $\epsilon_a'=5$, $\sigma_a=10^{-6}\,\mathrm{Sm}^{-1}$ and $\epsilon_b'=2$, $\sigma_b=10^{-8}\,\mathrm{Sm}^{-1}$ (dot-dashed line), $10^{-10}\,\mathrm{Sm}^{-1}$ (dotted line), or $10^{-11}\,\mathrm{Sm}^{-1}$ (solid line), respectively.

The plots of $\log(\epsilon_m'')$ versus $\log(\omega)$ display subtle differences in the low-frequency region. In Fig. 8(b) ($V_a=0.05$), when $\sigma_b=10^{-11}\,\mathrm{Sm}^{-1}$, an obvious peak can be observed on the curve of $\log(\epsilon_m'')$ versus $\log(\omega)$; when $\sigma_b=10^{-8}\,\mathrm{Sm}^{-1}$, however, the peak disappears; and the plot of $\log(\epsilon_m'')$ versus $\log(\omega)$ for $\sigma_b=10^{-10}\,\mathrm{Sm}^{-1}$ can be regarded as a transition stage in this evolution. In Fig. 9(b) ($V_a=0.10$), similar peaks and evolution processes can also be observed. However as V_a increases, these differences becomes less noticeable. When $V_a\geqslant 0.15$ [Figs. 10(b)–13(b)], the features become insignificant for the $\log(\epsilon_m'')$ versus $\log(\omega)$ plots. When $V_a\geqslant 0.5$ [Figs. 12(b)–13(b)], the plots of $\log(\epsilon_m'')$ versus $\log(\omega)$ for different σ_b values become undistinguishable. In the high-frequency region, $\log(\epsilon_m'')$ values all decrease linearly with the increase of $\log(\omega)$ [Figs. 8(b)–13(b)]. It is interesting to note that the slope of all these lines is a constant -1.0 demonstrating that ϵ_m'' is inverse proportional to ω in the high-frequency region.

The composites in this article are assumed to consist of cubic grains. Simulation of complex dielectric constants of composites consisting of irregular grains is in progress and will be the subject of our next publication.

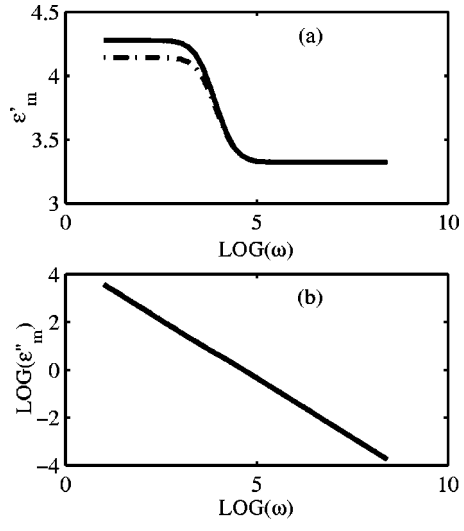

FIG. 12. Dielectric spectra of the composite at $V_a=0.50$ calculated by MC-FEM for $\epsilon_a'=5$, $\sigma_a=10^{-6}\,\mathrm{Sm}^{-1}$ and $\epsilon_b'=2$, $\sigma_b=10^{-8}\,\mathrm{Sm}^{-1}$ (dot-dashed line), $10^{-10}\,\mathrm{Sm}^{-1}$ (dotted line), or $10^{-11}\,\mathrm{Sm}^{-1}$ (solid line), respectively.

V. CONCLUSION

Complex dielectric constants of binary-phase random composites are simulated on a three-dimensional structure consisting of cubic grains using a Monte Carlo-finite element method. The permittivity and ohmic conductivity of the two phases are assumed to be frequency independent, i.e., interfacial polarization is the only polarization mechanism considered. Numerical results are fitted using Maxwell–Garnett, Bruggeman symmetrical, and general effective media formulas, and the fitting efficiencies of the formulas are quantitatively evaluated. The general effective media formula gives the best fits to our simulation results with a fitting accuracy better than 3.7%. In the low-frequency region, potential contours tend to avoid passing through one phase in the composite; in the high-frequency region, however, the period of time is too short for charge accumulation near the interphase boundaries.

[1] E. Tuncer, Y. V. Serdyuk, and S. M. Gubanski, IEEE Trans. Dielectr. Electr. Insul. **9**, 809 (2002).
[2] B. Sareni, L. Krahenhuhl, A. Beroual, and C. Brosseau, J. Appl. Phys. **80**, 1688 (1996); **80**, 4560 (1996); **81**, 2375 (1997); C. Brosseau, A. Beroual, and A. Bouaida, *ibid.* **88**, 7278 (2000).
[3] I. Krakovsky and V. Myroshnychenko, J. Appl. Phys. **92**, 6743 (2002).
[4] E. Tuncer, Ph.D. thesis, Chamers University of Technology, Gothenburg, Sweden, 2001.
[5] C. Ang, Z. Yu, R. Guo, and A. Bhalla, J. Appl. Phys. **93**, 3475 (2003).
[6] J. Jin, *The Finite Element Method in Electromagnetics* (Wiley, New York, 1993).
[7] I. Webman, J. Jortner, and H. Cohen, Phys. Rev. B **15**, 5712 (1977).
[8] L. K. H. van Beek, Prog. Dielectr. **7**, 69 (1967).
[9] P. N. Sen, C. Scala, and M. H. Cohen, Geophysics **46**, 781 (1981).
[10] F. Brouers, J. Phys. C **19**, 7183 (1987).

[11] C. Brosseau and A. Beroual, Prog. Mater. Sci. **48**, 373 (2003).
[12] J. W. Essam, C. M. Place, and E. H. Sondheimer, J. Phys. C **7**, L258 (1974).
[13] T. J. Coutts, Thin Solid Films **38**, 313 (1976).
[14] D. S. McLachlan, J. Phys. C **19**, 1339 (1986).
[15] D. J. Bergman and D. Stroud, in *Solid State Physics*, edited by H. Ehrenreich and D. Turnbull (Academic, San Diego, 1992), pp. 147–269.
[16] K. Lichtenecker, Phys. Z. **27**, 115 (1926).
[17] D. S. McLachlant and J. Chen, J. Phys.: Condens. Matter **4**, 4557 (1992).
[18] Y. Yuan, *Numerical Method For Nonlinear Programming* (Shanghai Scientific and Technical, Shanghai, 1993) p. 207.